

Wetting of anisotropic sinusoidal surfaces - experimental and numerical study of directional spreading

G. Fischer^{1,2}, M. Bigerelle¹, K.J. Kubiak^{*2}, T.G. Mathia³, Z. Khatir⁴, K. Anselme⁵

¹LAMIH, CNRS, Université de Valenciennes, France

²School of Engineering, University of Liverpool, Liverpool, UK

³Ecole Centrale De Lyon, LTDS CNRS UMR-5513, Ecully, France

⁴School of Engineering and Science, Curtin University - Sarawak, Miri, Malaysia

⁵Institut de Chimie des Surfaces et Interfaces, UPR CNRS 9069, Mulhouse, France

*E-mail: kris@kubiak.co.uk // k.kubiak@liverpool.ac.uk

Abstract

Directional wettability, i.e. variation of wetting properties depending on the surface orientation, can be achieved by anisotropic surface texturing. A new high precision process can produce homogeneous sinusoidal surfaces (in particular parallel grooves) at the micro-scale, with a nano-scale residual roughness five orders of magnitude smaller than the texture features. Static wetting experiments have shown that this pattern, even with a very small aspect ratio, can induce a strong variation of contact angle depending on the direction of observation. A comparison with numerical simulations (using Surface Evolver software) shows good agreement and could be used to predict the fluid-solid interaction and droplet behaviour on textured surfaces. Two primary mechanisms of directional spreading of water droplets on textured stainless steel surface have been identified. The first one is the mechanical barrier created by the textured surface peaks, this limits spreading in perpendicular direction to the surface anisotropy. The second one is the capillary action inside the sinusoidal grooves accelerating spreading along the grooves. Spreading has been shown to depend strongly on the history of wetting and internal drop dynamics.

Keywords: anisotropic surface, texture, wetting, high precision surface manufacturing, Surface Evolver

1. Introduction

Surfaces, whether natural or engineered, often exhibit an anisotropic roughness, i.e. some properties of the micro-topography vary with respect to the evaluation direction [1]. Researchers have shown a particular interest in measuring and quantifying surface anisotropy [2]. This interest is driven by the fact that a large number of designed engineered surfaces are anisotropic (due to fabrication processes, like cutting, or polishing [3, 4]), also because new micro-fabrication processes allows controlling the topographical pattern of a surface at a micro [5, 6] and nano-scale [7]. Trumpold et al. [8] have described the production method and use of calibration standards for roughness evaluation down to nanometre scale including a sinusoidal profile. Their design is based on

injection moulding of plastics negatives with different shapes (sinusoidal, triangular, step height). The fabrication methods of primary calibration standards includes ion-beam and plasma etching, sinus structures are obtained by holographic method of two beams interference exposure and by ultra-precision diamond cutting. The replication process shows very small influence on quality and precision of obtained surfaces. More general description of nanometre scale standard production methods for 3 orthogonal axes for scanning probe microscopes can be found in [9].

The anisotropy can induce very interesting properties to a surface, especially in terms of the surface wettability. Tailoring a surface with parallel structures can be an example, it has been shown [7-12] that a drop spreads preferably along the grooves, resulting in an elongated shape with a large difference

in terms of contact angle, depending on the direction of the drop observation. The most commonly used models of wetting on rough and nonhomogeneous surfaces, Wenzel's [13] and Cassie-Baxter's models [14], cannot predict directly the variations of contact angle when the surface is anisotropic [5,11], especially when the size of the drop has the same order as the size of the texture [10]. The sharp grooves obtained by Hans *et al.* [5] on copper alloys makes the contact angle vary along the drop contact line, with a difference up to 25% (from 75° to 95° approximately) for parallel and perpendicular direction of observation respectively.

Kusumaatmaja *et al.* [10] have shown a similar behaviour with periodically corrugated surfaces. Besides, the authors compared the experimental results with a numerical simulation, which in particular could predict the "pinning" of the three-phase line. Indeed, the experimental equilibrium shape of a drop has been shown to depend on its history: both when advancing and receding, the three-phase line can be pinned onto the edges of the micro-topography. The contact line pinning also observed in the case of a smooth but chemically patterned surface, [15, 16] is one explanation of the wetting hysteresis, and can be related to the existence of "metastable" states, described by A Marmur [17]. A drop placed on a complex surface can assume numerous metastable shapes, separated by energy barriers, the contact angle may thus take several values in the range limited by the advancing and receding contact angle, giving a thermodynamic explanation of the wetting hysteresis.

It is also possible to tailor the wettability by a multidirectional surface anisotropy, i.e. patterns composed of several primary directions, as it has been done by Vrancken *et al.* [18]. Hence, the authors managed to obtain droplets adopting polygonal-like footprints. An early study by Huh and Mason [19] also solved the Young-Laplace equation with an approximate perturbation method, in order to find the equilibrium shape of a drop sitting on a rough surface, notably in the particular case of a 3D sinusoidal surface. Their results showed for instance the phenomenon of capillary action known as "capillary channelling", i.e. the favoured moving of the three-phase line in the valleys of the texture, that they also observed experimentally [20].

This study will focus on experimental analysis of droplets behaviour on anisotropic surfaces. The surface texture was prepared in a form of unidirectional sinusoid on stainless steel surface, resulting in high quality anisotropic surfaces. A new method of surface texturing was developed and applied to a solid-liquid interface analysis. Experimental results are numerically modelled using Surface Evolver software. The aim is to create a framework for anisotropic surface analysis, numerical modelling and prediction

of droplet behaviour on complex and non-uniform surfaces. This will provide a set of tools for controlled and directional wettability design of functional surfaces.

Table 1. Geometrical description of the sinusoid textured samples.

Sample	Period (μm)	Peak to peak height R_z (μm)	Theoretical roughness factor ^a
SA4	100.0	4.0	1.004
SA8	100.0	8.0	1.016

^aRatio between the real surface and the projected one

2. Methods: experimental analysis and numerical modelling

2.1 Experimental setup

Stainless steel samples with precisely manufactured sinusoidal texture were used in order to compare numerical simulation with wetting experiments. The patent concerning the manufacturing process used to produce the samples is currently pending, and will be subject to future publication. Nevertheless, topographical measurements on prepared surfaces have been undertaken by tactile profilometry (*KLA-Tencor* profilometer), white light interferometry (*Zygo* interferometer) and atomic force microscopy (*Veeco* AFM). The wetting experiments were carried out using two sinusoidal samples, referred to as SA4 and SA8 (the names relate to the sinusoid amplitude), geometrical details are presented in table 1 and described in the next section.

2.1.1 Topographical characterization of the sinusoidal samples

The sinusoidal macroscopic shape is evaluated by tactile profilometry on a grid of 5mm x 50μm. As it can be observed in figure 1, there is no wave at a scale larger than the sinusoid, meaning that our process is well controlled at the macroscopic scale.

We now test the accuracy of the manufacturing process to well reproduce the shape of the sinus. To this aim, we compare 2D measurements of single period lengths of the sinus with a sinus curve fitted by a least square method, as shown in figure 2. Residuals from ideal sinus are plotted as the histograms in figure 3.

As it can be observed from the empirical probability density functions on figure 3, form error from ideal sinus is around 50nm for the 4μm sample and 150nm for the 8μm sample: these errors correspond approximately to 1-2% of the sinus amplitude. It must be noticed that these values include both lateral and vertical form error from an ideal sinus shape. However, these errors are correlated in the space and cannot be considered as a roughness but rather a discrepancy from an ideal sinus shape.

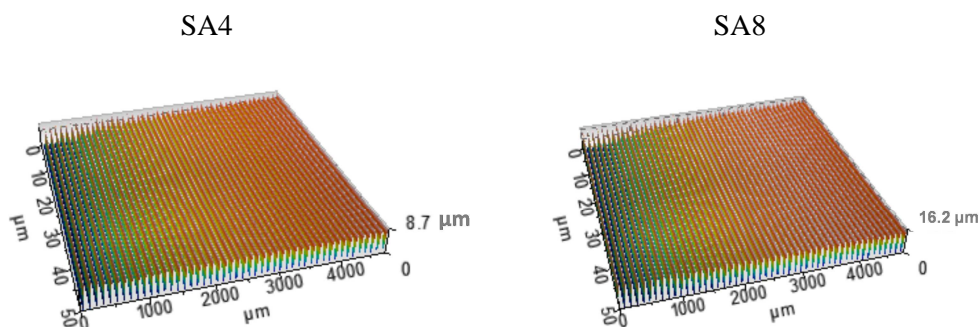


Figure 1. 3D measurement obtained by tactile profilometry on both surfaces: SA4 and SA8 with sinus amplitude of 4 and 8 μm respectively.

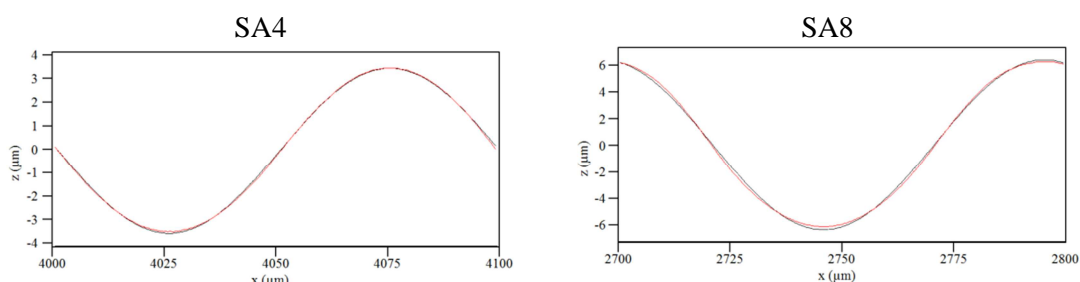


Figure 2. 2D extraction, by tactile profilometry, of a period on the surface. The red line represents the real surface and the black one the sinusoidal fit obtained by least squares method.

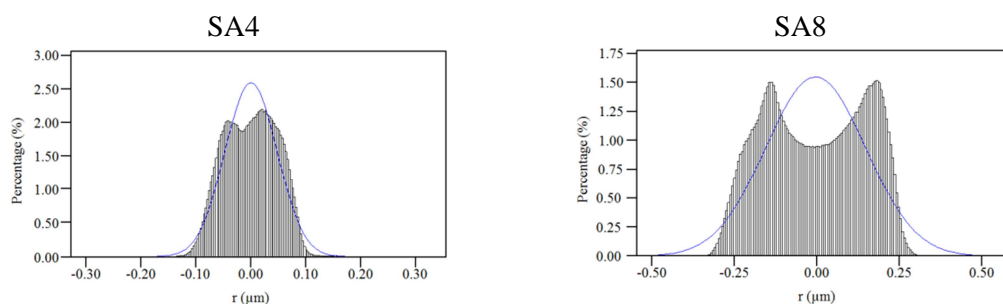


Figure 3. Histograms of the error on sinus amplitude obtained from 2D profile extraction (similar to these on figure 2), and empirical probability density (solid blue line).

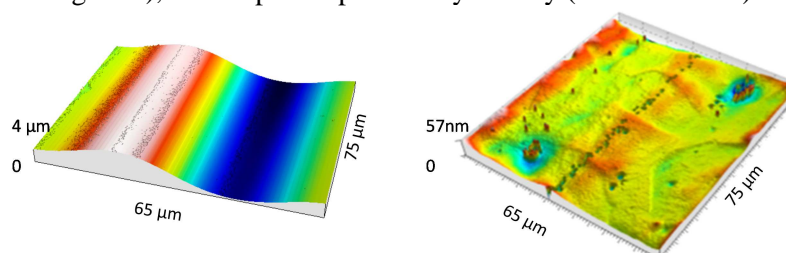


Figure 4. Results of interferometric measurements of sinusoidal surface over one period (left) and zoom of nano-roughness structure (right).

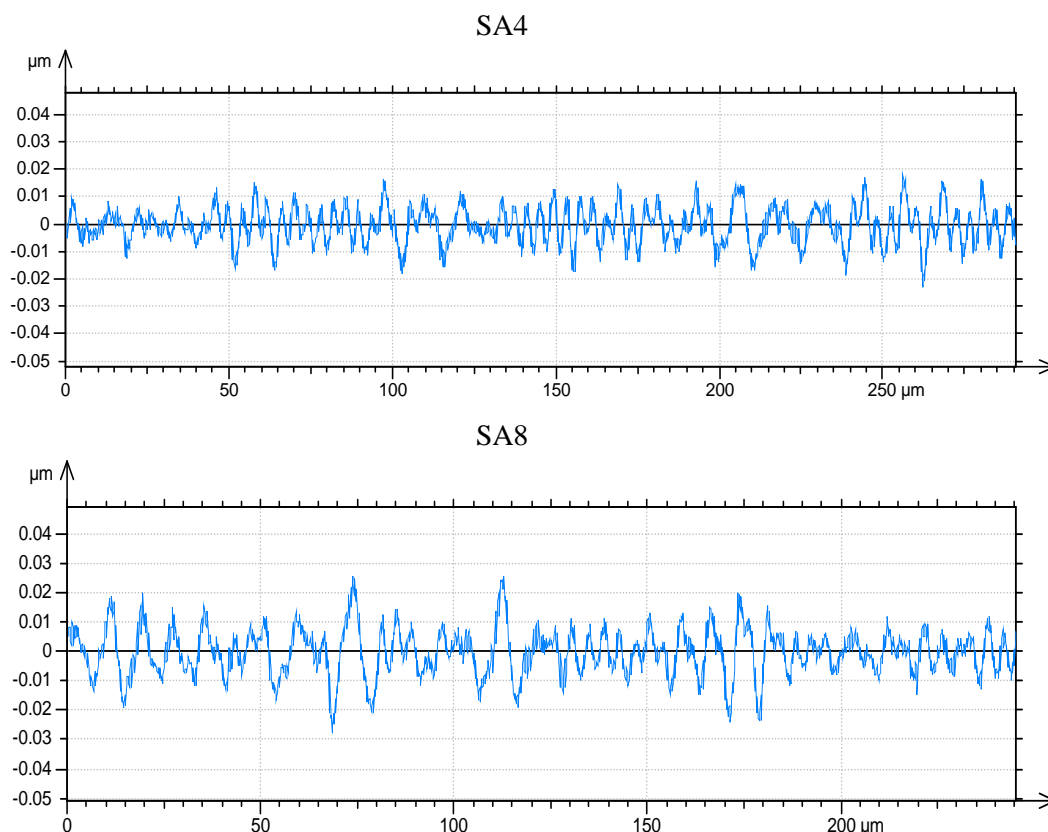


Figure 5. 2D measurement obtained by tactile scanning, after sinus form removal

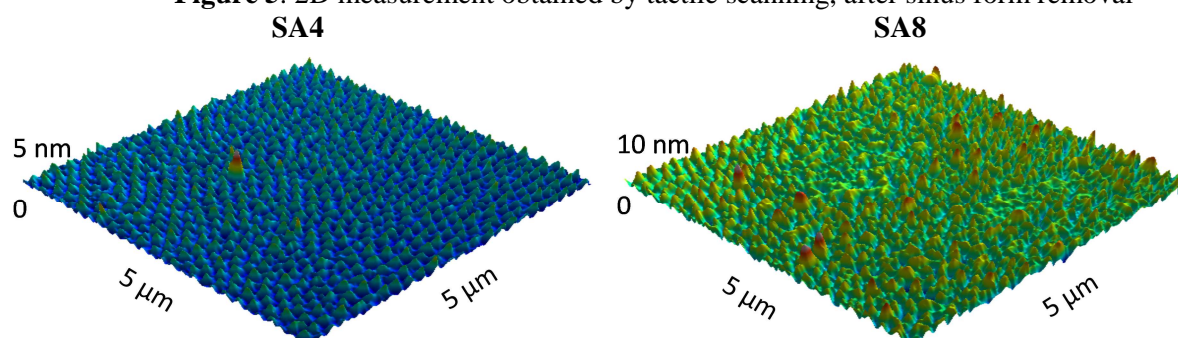


Figure 6. AFM measurement of the sinusoidal surfaces (5μm x 5μm grids), SA4 (left) and SA8 (right)

To quantify the nano-roughness, i.e. superimposed roughness at a scale smaller than the sinus, different techniques will be used. The major difficulty in terms of optical measurements is the high amplitude of the roughness, introducing high slopes that directly disturb the measurements. Figure 4 represents errors obtained from interferometric measurements. On the left hand side, one can see that error is overestimated in the inflexion points of the sinus (highest slope) and in some particular directions (AFM measurements confirm that it is an artefact). The zoom shown on the right hand side of the figure 4 clearly shows the grain size structure of the stainless steel presenting, of course, a nanometric amplitude. By evaluating more than 500 topographical measurements, in the zone without artefacts, we estimate a value of arithmetic

mean height of roughness to be 2 nm (S_a as defined by the ISO-25178 standard).

The sinusoidal microscopic form can be removed from stylus profilometry measurements (see 2D profiles on figure 5) in order to evaluate the surface roughness, the value of S_a obtained here is around 5 nm. Finally, AFM images obtained on a 5μm x 5μm grid (on figure 6) after form removal gives S_a around 2nm and S_{al} (shortest autocorrelation length) around 50nm.

To summarize, our new fabrication process allows us to create sinusoidal surfaces with amplitude around 10μm and without introducing waviness on a square of 5mm x 5mm. The form error from an ideal sinus wave is around 50nm and the residual nano-roughness is around 2nm (vertical error is less than 1/1000) with an autocorrelation length of 50nm for a

sinus wavelength of 100 μ m (lateral error is around 1/20000).

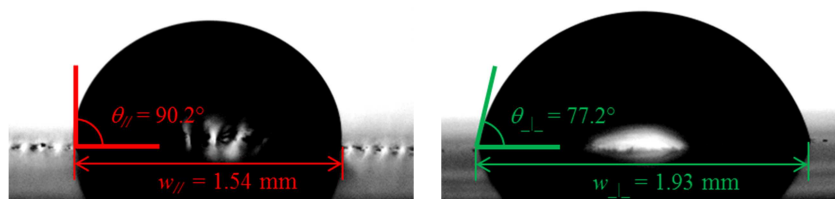


Figure 7. Example of anisotropy influence on apparent contact angle for parallel view (left) and perpendicular view (right) of a sessile drop (volume $\sim 1\mu$ L) deposited onto the SA8 sample.

Table 2. Experimental design for the wetting measurements analysis

Drop size	Volume ^a (μ L)	Number of drops per sample	Number of side views in each direction	Number of top views
Small drop	0.32 ± 0.05	12	6	12
Medium drop	1.3 ± 0.1	6	6	6
Big drop	11.6 ± 0.6	6	6	6

^aThe volume was computed in post-treatment step as the drop dispenser was controlled by a micrometric screw (not graduated in volume).

2.1.2 Wetting measurements

A MotionBLITZ EoSens® Mini camera (Mikrotron, Unterschleißheim, Germany) with microscopic lens (10x) was used to capture side view shadow-graphic pictures, as presented on figure 7, of the sessile drop, with a resolution of 1280x1024 pixels. A digital microscope with an adjustable magnification from 25x to 250x was also used to take top view photos of the sessile droplets, with a resolution of 2560x1920 pixels. Distilled water was used to generate the microliter droplets. Water drops were dispensed and slowly deposited onto the samples. Then, side views and top views of the drop were taken by both cameras. Measurements were made by analysis of the pictures, and focus on the contact angles and the contact width (width of the solid-liquid interface) for each view direction. The experiments were made at room temperature 20°C and 45% of relative humidity.

The series of measurements have been carried out on two samples with two different sinus amplitudes and with three different drop volumes, as presented in the table 2. The “Small” drops corresponded to the minimum volume that could be deposited with the micrometric syringe dispenser used in this study, and with the highest relative uncertainty, so that we have doubled the number of “Small” drops in order to get statistically consistent measurements. Mean values of contact angle was calculated from several experiments (see table 2), the uncertainties are calculated with a confidence of 95%.

Finally, it should be noted that previous wetting experiments have shown that the intrinsic contact angle for sessile water drops on a not textured sample of stainless steel was $\theta_i = 75^\circ$, which is rather hydrophilic. This value will be used in the simulation.

2.2 Surface Evolver software

Surface Evolver has been developed by K A Brakke from the Department of Mathematics of the Susquehanna University, Pennsylvania, USA. This tool computes the minimal energy shape of a 3D surface mesh under constraints. A full description of the theory lying behind the Surface Evolver is available in [21]. We will only remind a few basic concepts that are useful for the comprehension of the simulation.

Surface Evolver basically represents a system as a ‘simplicial complex’, i.e. a discrete finite mesh composed of vertices and edges defining oriented triangular facets in a three-dimensional space. Any element of the mesh can be constrained (at a given position or with a specified surface tension for instance) and all of the constraints are converted as a global energy of the mesh. The initial mesh and constraints have to be defined by the user (an example of initial file is given in appendix A.1).

In order to find the minimum energy associated with mesh, the basic operation of the program is an iteration step, during which each vertex is moved and system energy is evaluated. After each step, the global energy of the mesh decreases, tending to a steady state value.

Surface Evolver has been used by several authors to study capillarity driven phenomena [22, 23], droplet-shapes onto chemically heterogeneous [24] or rough surfaces [25, 26]. Brandon *et al.* [24] used Surface Evolver to simulate a sessile drop onto a chemically patterned surface. The model implied a flat substrate with a surface tension evolving as a sinusoidal function along a single direction. The resulting surface was thus made by parallel stripes with alternating hydrophobic/hydrophilic regions. Their simulation has shown how the contact angle varies

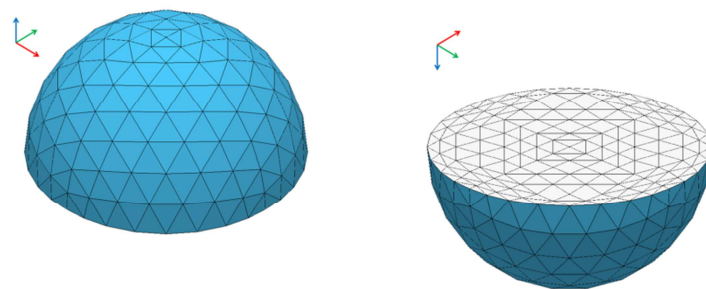


Figure 8. Initial geometry (hemisphere approximated by 524 facets) for the Surface Evolver simulation, isometric view from the top (left) and from the bottom (right). The blue facets belong to the liquid-vapour interface (I_{LV}) whereas the white ones belong to the solid-liquid interface (I_{SL})

Table 3. Experimental results of wettability analysis (mean values)

Sample	Drop size	Contact Angle ($^{\circ}$)			Drop width (mm)		Elongation ratio ($w_{\perp} - w_{\parallel}$)/ w_{\perp}
		θ_{\parallel}^a	θ_{\perp}	$\theta_{\parallel} - \theta_{\perp}$	w_{\parallel}	w_{\perp}	
SA4	Small	82.0 ± 4.5	74.5 ± 5.0	8	1.15 ± 0.12	1.15 ± 0.11	0 %
	Medium	87.5 ± 9.0	76.0 ± 6.0	12	1.72 ± 0.08	1.91 ± 0.09	11 %
	Big	85.0 ± 7.5	74.0 ± 5.5	11	3.71 ± 0.20	4.14 ± 0.09	11 %
SA8	Small	91.5 ± 7.0	78.0 ± 7.5	13	1.04 ± 0.17	1.12 ± 0.12	8 %
	Medium	96.5 ± 6.5	80.5 ± 5.5	16	1.53 ± 0.09	1.86 ± 0.08	21 %
	Big	95.0 ± 3.5	82.5 ± 4.5	13	3.43 ± 0.20	4.07 ± 0.16	18 %

^a θ_{\parallel} correspond to the contact angle measured in the parallel view (see figure 9).

around the drop, and that its final shape depends on its history (leading to the definition of advancing and receding contact angles). Patankar and Chen [25] modelled the equilibrium shape of a drop onto a surface made of horizontal square grooves.

The authors considered both the Wenzel and Cassie-Baxter state, and managed to identify a threshold contact angle splitting the two cases. Promraksa and Chen [26] also used Surface Evolver to show the multiple metastable states on a cosine square pattern for a drop in a Wenzel state, and used these metastable states to predict the advancing and receding contact angles.

The drop is modelled in the 3D space as the union of a solid-liquid interface (I_{SL}) and a liquid-vapour one (I_{LV}). During the computation, the vertices belonging to I_{SL} are constrained to stay on the sinusoidal surface, thus assuming a Wenzel state. The coordinates of the vertex belonging to the I_{LV} are not constrained. It should be noted that some vertices belong to both interfaces: the three-phase line. The surface tension is parameterized by the intrinsic contact angle θ_i (by convention expressed in degrees): the surface tension of facets belonging to I_{LV} is set to 1, whereas the tension of facets in I_{SL} is $-\cos(\pi\theta_i/180)$. The effect of the gravity is negligible in this case and do not influence the results significantly therefore, it was not taken into account in our model.

Our initial geometry is an approximate hemisphere which is presented in figure 8.

The equilibrium shape of the numerical simulation will be computed by successive refinements

and energy minimization steps. The discrete mesh has to approximate a sinusoidally curved surface. One of the most important parameters in wetting on textured surface is the roughness ratio (ratio between the real surface area and the projected one), used in Wenzel's model. However, the period of the surface sinusoid is large compared to its amplitude, the theoretical roughness ratio is thus close to unity, and it has been observed that the roughness ratio of the simulation mesh quickly converges [27, 28] to the theoretical value.

3. Results and Discussion

3.1 Experimental results

The experiments have shown a strong influence of the surface anisotropic pattern on the shape of the sessile water droplets. The drops spread significantly more along the grooves of the surface than in the perpendicular direction, leading to an elongated final shape of the droplet (see table 3 and figure 9). Hence, the contact angle varies also along the droplet perimeter depending on the view direction: the contact angle obtained when observing in parallel direction to the grooves is between 8° to 16° larger than in the perpendicular direction. The ratio between the widths of the drop in both directions is also an indication on the anisotropy effect. The drops are from 10% to 20% (respectively for SA4 and SA8 sample) longer along the grooves than in the perpendicular direction, except in the case of the smallest droplets when elongation is less visible and only few grooves are covered.

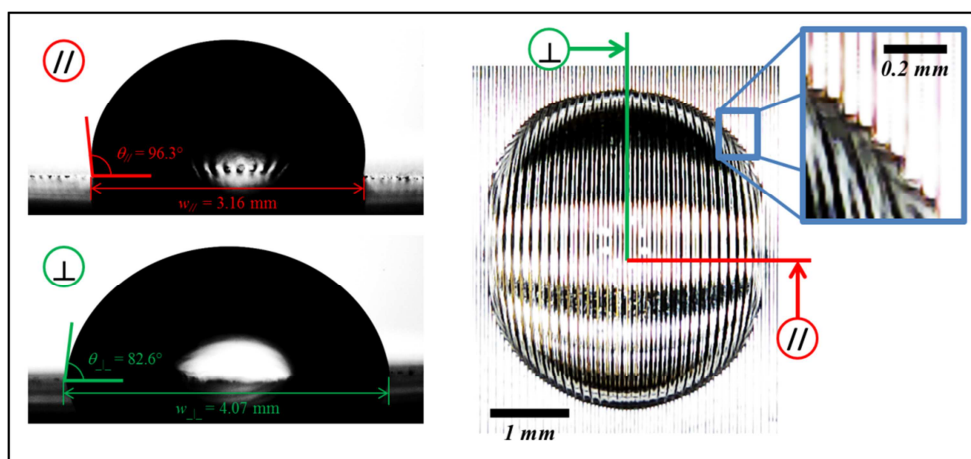


Figure 9. Side views in parallel and perpendicular direction and top view of a sessile “Big” drop on sample SA8.

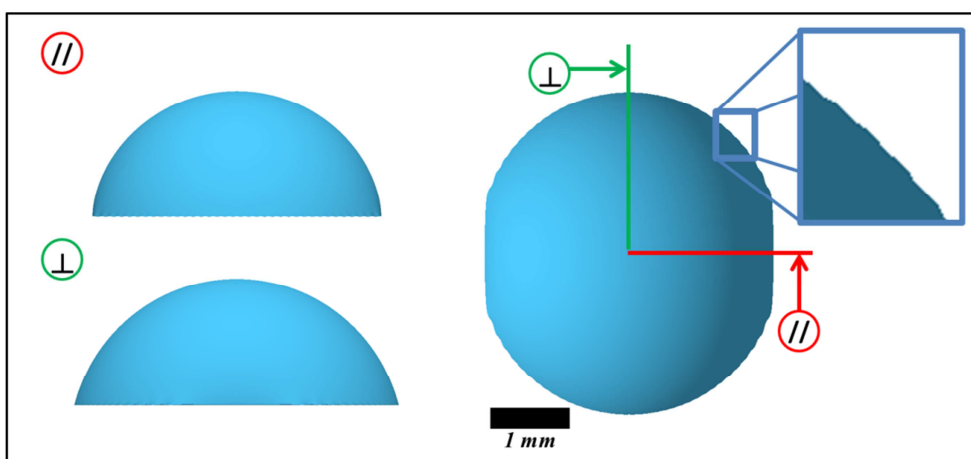


Figure 10. Side views in parallel and perpendicular direction and top view of a simulated sessile “Big” drop on the 8 μ m amplitude sinusoid. The contact angles are $\theta_{//} = 89.5^\circ$ and $\theta_{\perp} = 76.0^\circ$.

Table 4. Numerical results of surface anisotropy influence on wettability

Sample	Drop size	Angles ($^\circ$)			Drop widths (mm)		Elongation ($w_{\perp} - w_{//}$)/ w_{\perp}	Number of grooves ^a
		$\theta_{//}$	θ_{\perp}	$\theta_{//} - \theta_{\perp}$	$w_{//}$	w_{\perp}		
SA4	Small	75.0	76.0	-1.0	1.20	1.17	- 2%	12
	Medium	81.5	76.0	5.5	1.84	1.93	5 %	18
	Big	81.5	76.0	5.5	3.84	4.01	4 %	38
SA8	Small	88.0	75.5	12.5	1.05	1.21	15 %	10
	Medium	85.5	75.5	10.0	1.82	1.94	7 %	18
	Big	89.5	76.0	13.5	3.64	4.06	12 %	38

^aEffective number of grooves on which the virtual drop is lying.

Moreover, the difference between the mean contact angles in each direction increases with the amplitude of the sinusoid: greater the amplitude, greater the anisotropic effect.

When the droplet is deposited onto a textured sinusoidal surface two different effects will contribute to influence the contact angle and the contact line.

The first one is a mechanical barrier created by the peaks of sinus surface limiting the spreading beyond the next peak. At the same time the second effect is the capillarity action along the surface grooves

which will enhance the spreading of liquid in this direction. Note that higher amplitude will limit mainly spreading in perpendicular direction whereas smaller period of sinusoidal surface will mainly accelerate the capillary action.

Another interesting effect which can be observed experimentally is a discrete contact line shape on a sinusoidal textured surface. As it can be observed on the zoomed part on a top view of droplet (Figure 9), contact line has clearly visible steps when contact line progresses from one groove to another

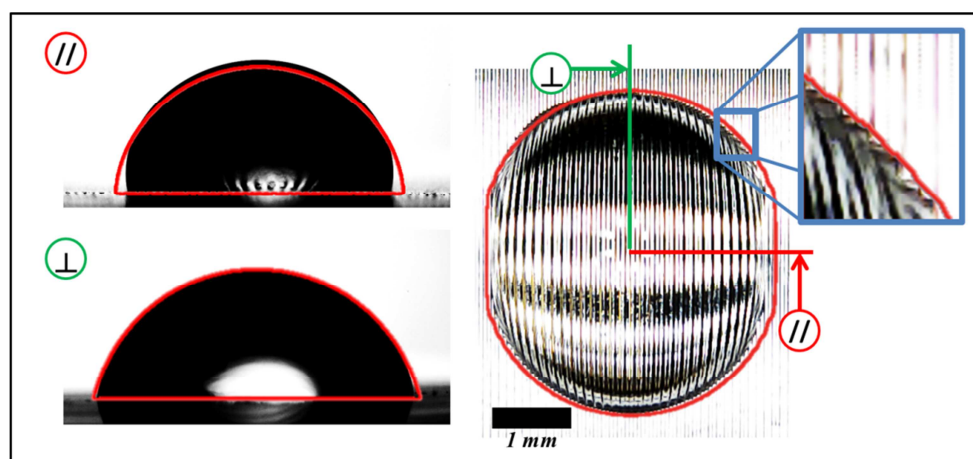


Figure 11. Comparison of numerical (Figure 10) and experimental results (Figure 9), red line represents numerical results.

rather than smooth continuous shape. This, on one hand confirms the capillary action taking place inside the grooves and it also shows the discrete character of the anisotropic surface interface.

3.2 Surface Evolver results

The developed here numerical model computed with Surface Evolver shows the preferential spreading along the grooves of the sinusoidal surface, as presented in figure 10 and in table 4, summarizing the numerical results. The contact angle in the perpendicular direction is almost constant for all simulations and is very close to 75° (the intrinsic contact angle of the simulated surface). The difference between the contact angles in both directions increases with the amplitude of the sinusoid pattern, with a maximum value of 13.5° . It should be noted that, using the same initial geometry for both amplitudes (4 and $8\mu\text{m}$), the virtual drop converges towards a shape where it sits on the same number of grooves, except for the “Small” drop. Indeed, for the $4\mu\text{m}$ amplitude, the drop lies on 12 grooves, even leading to a lower contact angle in the parallel direction than in the perpendicular one (figure 11).

Finally, we notice (see the zoomed area on the top view in figure 10) that the three-phase line oscillates in the grooves, but does not have the same shape as in the experimental case, on figure 9. Additional analysis preferably using alternative methods like Volume of Fluids or lattice Boltzmann will be required to explore this intriguing behaviour in more details.

Experiments have shown that, as expected, the liquid spreads preferably along the grooves of the surface and that the three-phase line seems to be pinned on the parallel peaks of sinusoidal texture. Besides, the phenomenon of capillary action can be observed on the top views: the capillarity accelerates the flow of the fluid in the grooves, increasing the elongation of the drop. Though the aspect ratio of the samples (amplitude divided by the period) is very

small for both samples 0.04 and 0.08 respectively, the drops are strongly affected, with a difference of contact angle up to 15 and 20% respectively.

The simulation shows a similar behaviour, for instance predicting that higher sinusoid amplitude increases the elongation of the drop and the contact angle variation. Good qualitative agreement has been obtained. Surface Evolver is capable of calculating a metastable state for a given drop deposited on a surface. It has been shown experimentally that the metastable state experienced by a drop depends on its history. Hence, even if we compute every metastable shape for a given volume onto a given textured surface, the numerical simulation would be very difficult or almost impossible to compare qualitatively with experiments due to its dynamic history, droplet generation and deposition method and experimental uncertainty of obtained results.

5. Conclusion

The paper explores influence of surface anisotropy on wettability and directional spreading of droplets on the textured sinusoidal surface. Experimental analysis of different size droplets deposited on two sinusoidal surfaces with amplitudes of $4\mu\text{m}$ and $8\mu\text{m}$ were compared with results of numerical simulations which were modelled using the Surface Evolver software. The experimental and the numerical results presented here leads to following conclusions:

- The surface anisotropy has strong influence on directional spreading and wettability,
- Droplet deposited on the anisotropic surface will form an elongated or an elliptical shape,
- Evidence of capillary action taking place inside the grooves was confirmed by experimental results,
- Mechanism of droplet elongation has been identified as a mechanical barrier for liquid to spread in direction perpendicular to the surface

anisotropy and capillary action taking place along the grooves leading to droplet elongation.

6. Perspectives

To explore discrete character of anisotropic wettability on sinusoidal surfaces experiments with even smaller droplets comparing to texture period could be carried out. Depending on the droplets size one can expect discrete metastable states to be visible and to be able to find the correlation between the history of dynamic evolution and a final steady state of the droplet on a surface.

Also the effect of capillary action creating the steps shape can be explored in details by varying the surface period or by using alternative numerical models.

Acknowledgements

The authors are grateful to Dr Jetinger Singh and Dr Kate Blake for granting us access to the *Mikrotron* high speed camera and for help in configuration of the experimental setup. This study was partially supported by the *Agence National de la Recherche* through the project “Sinus surf” ANR-12-BSV5-0010.

Appendix A. Surface Evolver (version 2.70) scripts

A.1 Computation of the initial geometry

The following script has been used to compute the initial geometry, an approximate hemisphere (comments are preceded by a double forward slash):

```
// Beginning of script
// Variable definition
parameter vol = 1e9 // drop volume (μm^3)
#define larg (3*vol)^(1/3)/sqrt(2) // width of the tetrahedron
base

parameter theta = 90 // intrinsic contact angle for the initial
geometry
#define Tls (-cos(theta*pi/180)) // surface tension on the
solid-liquid interface

// Sinusoidal surface parameters
parameter period = 100
parameter height = 0
parameter phi = 0
constraint sinus_surf
formula: z - cos(2*pi*x/period + pi*phi/180)*height/2 = 0

// Starting geometry definition (tetrahedron)
// all the elements corresponding to the solid-liquid interface
are constrained by “sinus_surf”
vertices
1 larg 0 0 constraint sinus_surf
2 0 larg 0 constraint sinus_surf
3 -larg 0 0 constraint sinus_surf
4 0 -larg 0 constraint sinus_surf
```

```
5 0 0 0 constraint sinus_surf
6 0 0 larg*sqrt(2)
edges
1 1 2 constraint sinus_surf
2 2 3 constraint sinus_surf
3 3 4 constraint sinus_surf
4 4 1 constraint sinus_surf
5 1 5 constraint sinus_surf
6 2 5 constraint sinus_surf
7 3 5 constraint sinus_surf
8 4 5 constraint sinus_surf
9 1 6
10 2 6
11 3 6
12 4 6
facet
// “tension” correspond to the surface tension
// set to two values depending on the interface (solid-liquid
or liquid-vapour)
1 1 10 -9 frontcolor lightblue
backcolor white tension 1
2 2 11 -10 frontcolor lightblue
backcolor white tension 1
3 3 12 -11 frontcolor lightblue
backcolor white tension 1
4 4 9 -12 frontcolor lightblue
backcolor white tension 1
5 -1 5 -6 color -1 constraint
sinus_surf tension Tls
6 -2 6 -7 color -1 constraint
sinus_surf tension Tls
7 -3 7 -8 color -1 constraint
sinus_surf tension Tls
8 -4 8 -5 color -1 constraint
sinus_surf tension Tls
body // the volume of the system is constrained
1 1 2 3 4 5 6 7 8 volume vol

// Computation
// “r” = refinement of the mesh
// “g” = iteration step
// “u” = mesh equiangularization
read
{r; g 100; u} 3 // numbers correspond to the repetitions
// End of script
```

A.2 Script for the computation on sinusoidal surfaces

Using the geometry obtained with the script in appendix A.1, and by modifying the intrinsic contact angle θ_i and the parameters (period, amplitude and phase) of the sinusoid, the following script – which has been found to optimize the ratio computation time / fineness of the mesh – can be used to evolve the system towards an equilibrium shape:

```
// beginning of script
r // refinement
{g 5;u;V} 50 // “g” = iterations, “u” = equiangularization, “V” =
vertex averaging
r
```

```
{g 5;u;V} 25
r
{g 5;u;V} 10
r
{g 5;u;V} 5
// end of script
```

References

- [1] Whitehouse D J 1994 Handbook of Surface Metrology IOP Pub. (Bristol, United Kingdom: Taylor & Francis)
- [2] Thomas T R, Rosén B-G and Amini N 1999 Fractal characterisation of the anisotropy of rough surfaces Wear 232, 41
- [3] Kubiak K J, Wilson M C T, Mathia T G and Carval P 2011 Wettability versus roughness of engineering surfaces, Wear 271, 523
- [4] Mathia T., Lanteri P., Longeray R., Midol A. 1988 Histoire d'une goutte de liquide isolant déposée sur une surface: influence de la topographie et de la physico-chimie, Le Vide, les Couches Minces, N° Special, October.
- [5] Hans M, Müller F, Grandthyll S, Hüfner S and Mücklich F 2012 Anisotropic wetting of copper alloys by one-step laser micro-patterning Appl. Surf. Sci. 263 416
- [6] Mathia T., Louis F., Maeder G., Mairey D. 1982 Relationships between surface states, finishing processes and engineering properties, Wear 83 241-250
- [7] Bizi-Bandoki P, Benayoun S, Valette S, Beaugiraud B and Audouard E 2011 Modifications of roughness and wettability properties of metals induced by femtosecond laser treatment Appl. Surf. Sci. 257(12) 5213
- [8] Trumpold, H., Frenzel, C., Chetwynd, D.G., Anghel, V., Konejung, K., Reitze, B., Preut3, W., Gessenharter, A., De Chiffre, L., Andreasen, J.L., Sammartini-Malberg, M.P., Rubert, P., Leach, R., Schreiter, S., Breger, P. 2001 Calibration standards for surface topography measuring systems down to the nanometric range, Final report on EC-project SMT4-CT97-2176
- [9] Garnaes, J., Kofod, N., Joergensen, J.F., Kuhle, A., Besmens, P., Ohlsson, O., Rasmussen, J.B., Lindelof, P.E., Wilk, G., Koenders, L., Mirande, W., Hasche, K., Haycocks, J., Nunn, J., Stedman, M. 2000, Nanometre scale transfer standards, Proc. X Int. Coll. Surf., Chemnitz, Germany 34-137
- [10] Kusumaatmaja H, Vrancken R J, Bastiaansen C W M and Yeomans J M 2008 Anisotropic drop morphologies on corrugated surfaces Langmuir 24 7299
- [11] Ma C, Bai S, Peng X and Meng Y 2013 Anisotropic wettability of laser micro-grooved SiC surfaces Appl. Surf. Sci. 284 930
- [12] Kubiak K.J., Mathia T.G., 2014 Anisotropic wetting of hydrophobic and hydrophilic surfaces - modelling by Lattice Boltzmann Method, Procedia Engineering, Elsevier (in press)
- [13] Wenzel R N 1936 Resistance of solid surfaces to wetting by water Ind. Eng. Chem. 28 988
- [14] Cassie A B D and Baxter S 1944 Wettability of porous surfaces Trans. Faraday Soc. 40 546
- [15] Gau H, Herminghaus S, Lenz P and Lipowski R 1999 Liquid morphologies on structured surfaces: from microchannels to microchips Science 283 47
- [16] Bliznyuk O, Jansen P, Kooij E S and Poelsema B 2010 Initial spreading kinetics of high-viscosity droplets on anisotropic surfaces Langmuir 26(9) 6328
- [17] Marmur A 1994 Thermodynamic aspects of contact angle hysteresis Advances in Colloid and Interface Science 50 121
- [18] Vrancken R J, Blow M L, Kusumaatmaja H, Hermans K, Prenen A M, Bastiaansen C W M, Broer D J and Yeomans J M 2013 Anisotropic wetting and de-wetting of drops on substrates patterned with polygonal posts Soft Matter 9 674
- [19] Huh C and Mason S G 1977 Effects of surface roughness on wetting (theroretical) Journal of Colloid and Interface Science 60(1) 11
- [20] Oliver J F, Huh C and Mason S G 1980 An experimental study of some effects of solid surface roughness on wetting Colloids and Surfaces 1 79
- [21] Brakke K A 1992 The surface evolver Experimental Mathematics 1 141
- [22] Collicot S H and Weislogel M M 2004 Computing existence and stability of capillary surfaces using Surface Evolver AIAA Journal 42(2) 289
- [23] Grzybowski B A, Bowden N, Arias F, Yang H and Whitesides G M 2001 Modeling of Menisci and Capillary Forces from the Millimeter to the Micrometer Size Range J. Phys. Chem. B 105 404
- [24] Brandon S, Wachs A and Marmur A 1997 Simulated contact angle hysteresis of a three-dimensional drop on a chemically heterogeneous surface: a numerical example Journal of Colloid and Interface Science 191 110
- [25] Patankar N A and Chen Y, Numerical simulation of droplet shapes on rough surfaces, Nanotech 2002 Vol. 1, p.116 - 119
- [26] Promraksa A and Chen L-J 2012 Modeling contact angle hysteresis of a liquid droplet sitting on a cosine wave-like pattern surface Journal of Colloid and Interface Science 384 172
- [27] Ramon-Torregrosa P J, Rodriguez-Valverde M A, Amirfazli A and Cabrerizo-Vilchez 2008 Factors affecting the measurement of roughness factor of surfaces and its implications for wetting studies Colloids and Surfaces A: Physicochem. Eng. Aspects 323 83
- [28] Kannan R, Vaikuntanathan V and Sivakumar D 2011 Dynamic contact angle beating from drops impacting onto solid surfaces exhibiting anisotropic wetting Colloids and Surfaces A: Physicochem. Eng. Aspects 386 36